

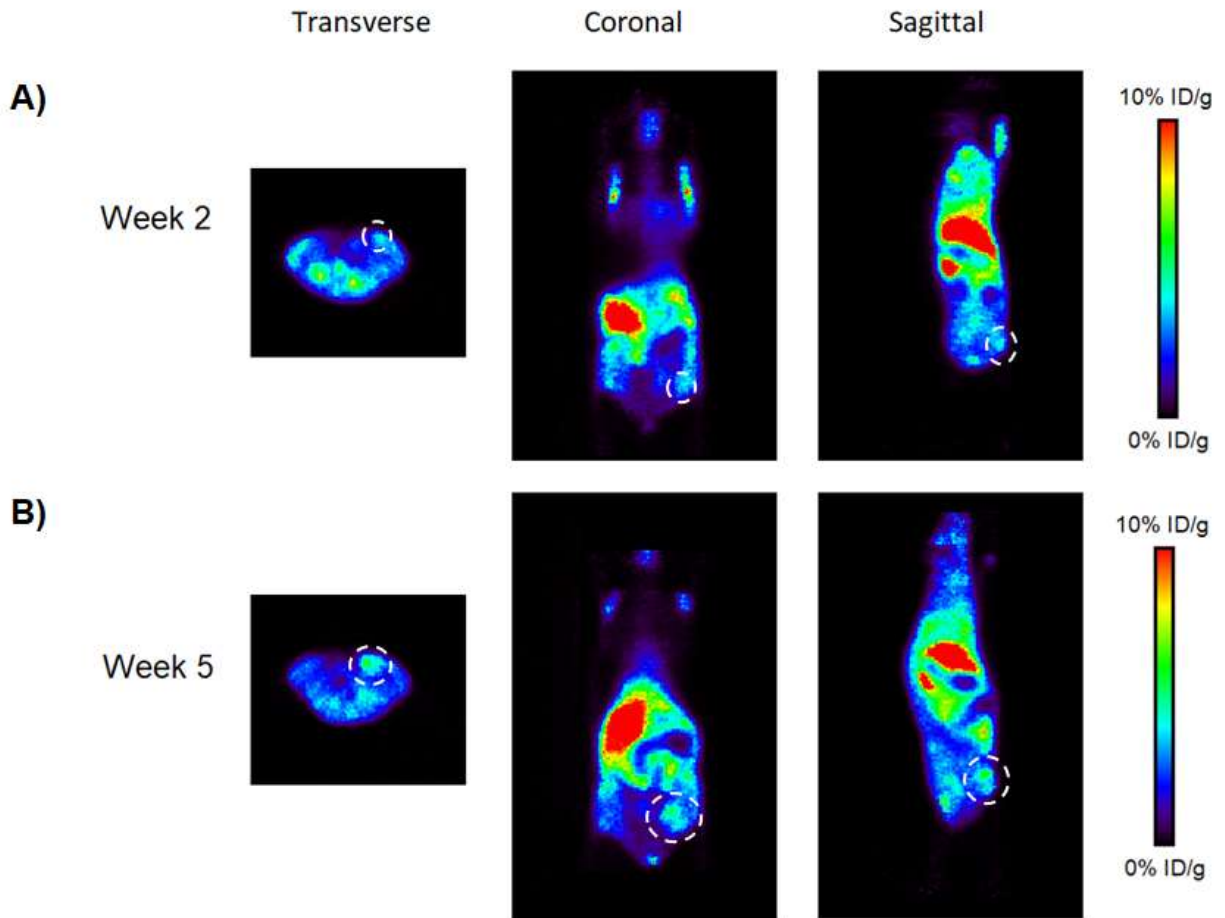
## Radiochemical synthesis

Desmethyl-PS13 and authentic PS13 were synthesized as previously described (17) and all other compounds were obtained from commercial sources. [ $^{11}\text{C}$ ]PS13 was prepared using a GE Tracerlab FX2 C-Pro<sup>TM</sup> synthesis module, as previously described (17), with minor modifications to adapt a “loop method” (19). Briefly, desmethyl-PS13 ( $1.0 \pm 0.1$  mg) was dissolved in dimethylformamide (80  $\mu\text{L}$ ) then 1.5  $\mu\text{L}$  of potassium *tert*-butoxide solution (1.0 M in tetrahydrofuran) was added. The resulting solution was injected onto a 5 mL stainless steel loop approximately 5 minutes prior to radiosynthesis. [ $^{11}\text{C}$ ]iodomethane transferred to the loop and held at room temperature for 5 min prior to high pressure liquid chromatography (HPLC) purification and formulation. [ $^{11}\text{C}$ ]PS13 was prepared to a molar activity of 11-101 GBq/ $\mu\text{mol}$  with >99% radiochemical purity.

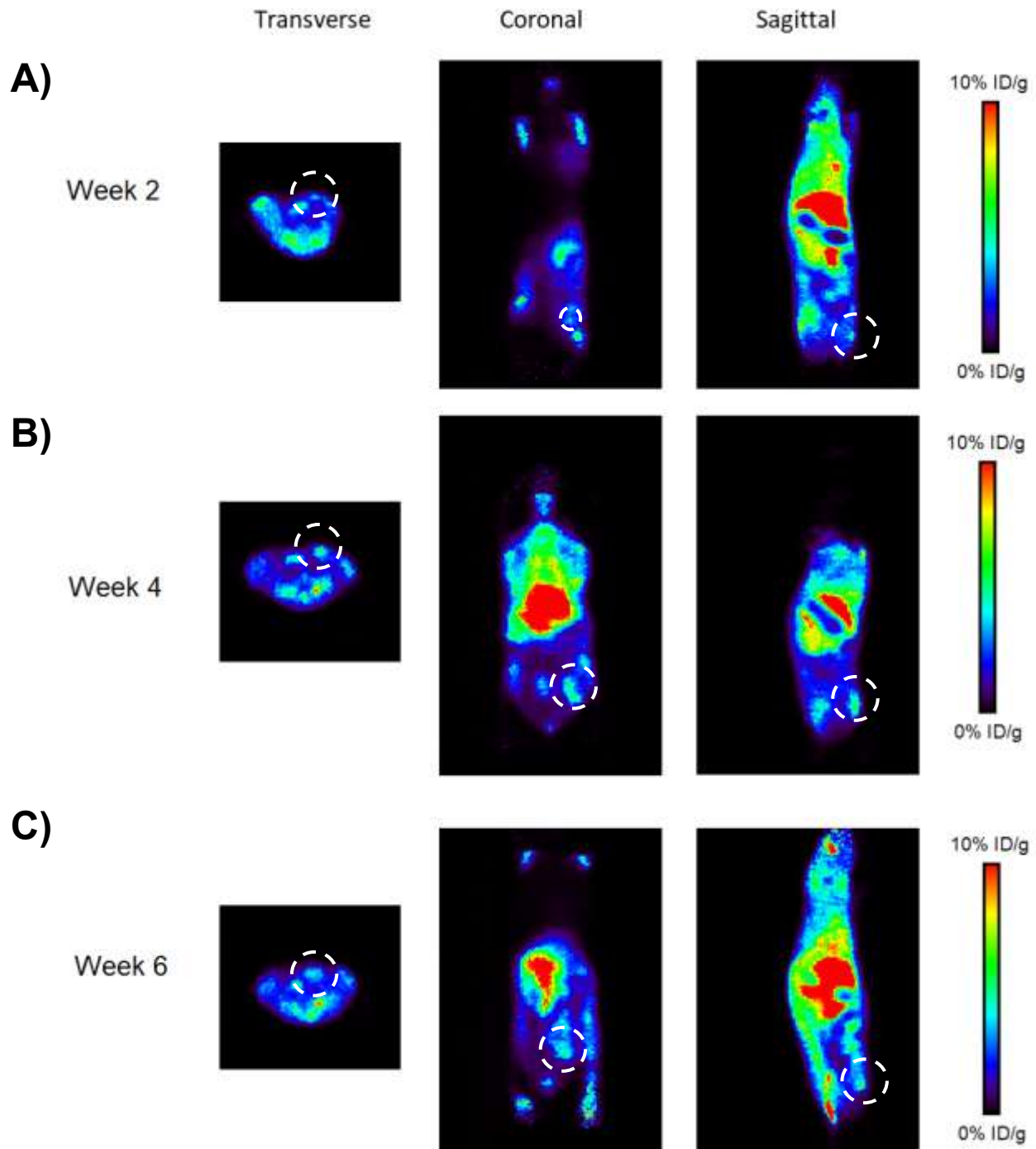
## PET/MR acquisition and analysis

*PET acquisition method:* With mice anesthetized and stable in the PET/MR scanner, a short gradient echo (GRE) scout MR was acquired for positioning the mouse in the PET field of view followed by a T1-weighted material map MR acquisition (GRE 3D, TR 25 ms, TE 4.76 ms) for PET and MR co-registration and PET scatter and attenuation corrections. PET scans were initiated at the time of radioligand injection and the list mode data were acquired for 60 min with an energy window of 400-600 keV.

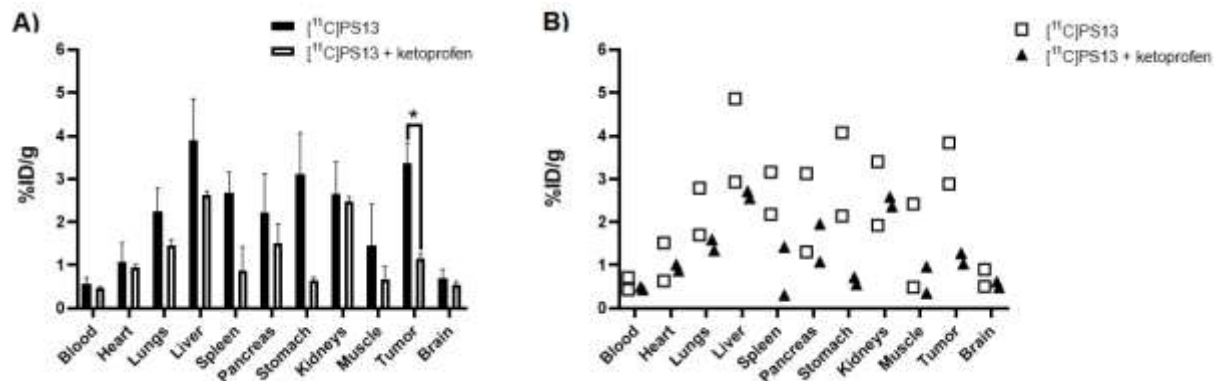
*PET data analyses:* Acquired data were sorted into 33, 3D (3 $\times$ 5s, 3 $\times$ 15s, 3 $\times$ 20s, 7 $\times$ 60s, 17 $\times$ 180s) true sinograms (ring difference 84). 3D sinograms were converted in 2D sinograms using Fourier rebinning (20) with corrections for detector geometry, efficiencies, attenuation and scatter, prior to image reconstruction using a 2D-filtered back projection (FBKP) with a Hann filter at a cut-off of 0.50  $\text{cm}^{-1}$ . A static image of the complete emission acquisition was reconstructed with the manufacturer's iterative 3D algorithm (6 subsets, 4 iterations). The static iterative image was used for PET and MR co-registration and for presentation in figures. All data were corrected for dead-time and decay corrected to the start of acquisition. Dynamic FBKP images were used to extract time-activity curves (TACs). Regions of interest (ROIs) were placed in the tumor or contralateral muscle tissue. TACs were extracted from ROIs and expressed as %ID/g, assuming tissue density of 1 g/mL.



**SUPPLEMENTAL FIGURE 1.** PET imaging of [ $^{11}\text{C}$ ]PS13 in an individual OVCAR-3 i.p. xenograft mouse (n=3). Transverse, coronal, and sagittal views of representative PET images, 0-60 min, at (A) week 2, and (B) week 5 post-inoculation.



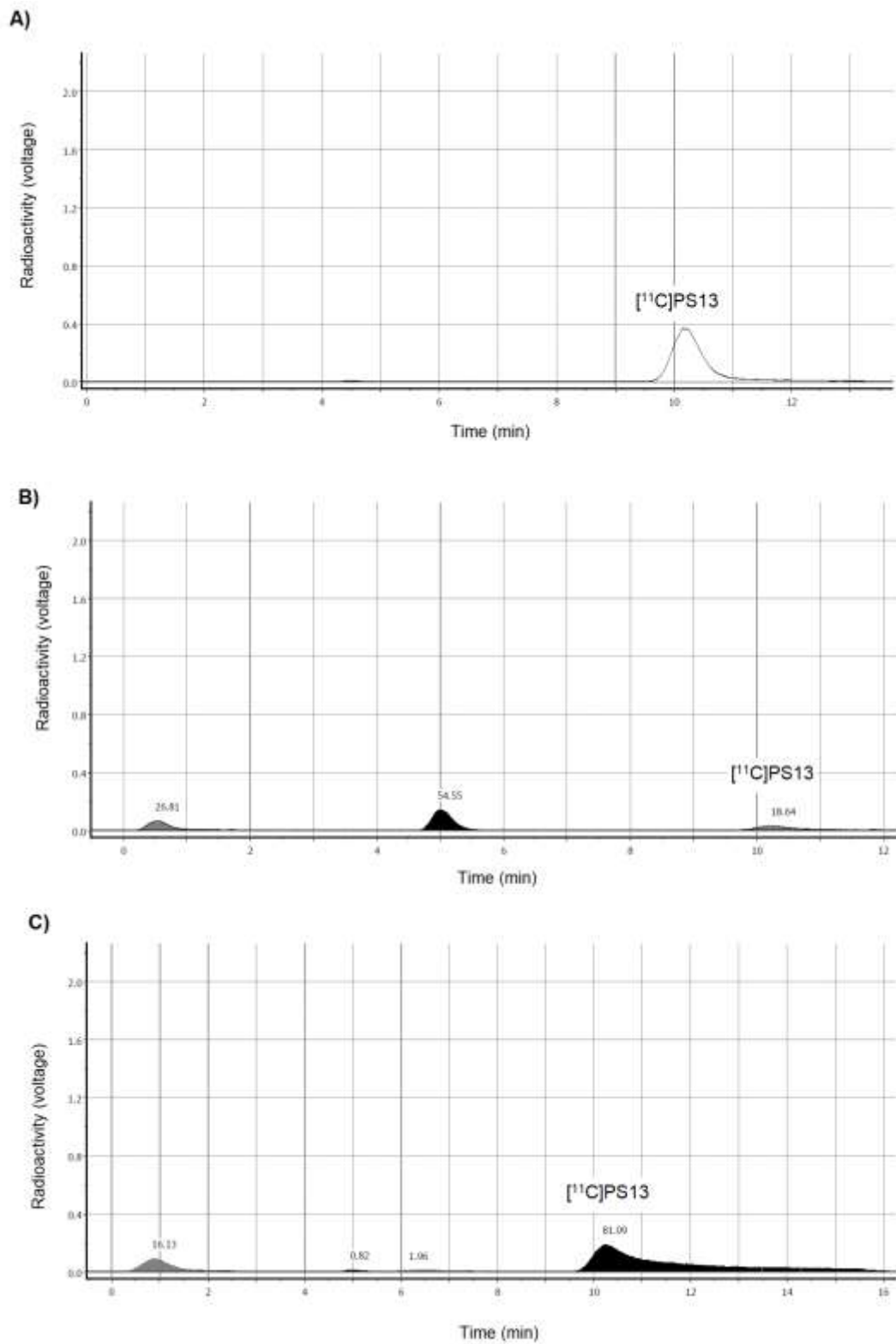
**SUPPLEMENTAL FIGURE 2.** PET imaging of  $[^{11}\text{C}]\text{PS13}$  in an individual OVCAR-3 i.p. xenograft mouse (n=3). Transverse, coronal, and sagittal views of representative PET images, 0-60 min, at (A) week 2, (B) week 4, and (C) week 6 post-inoculation.



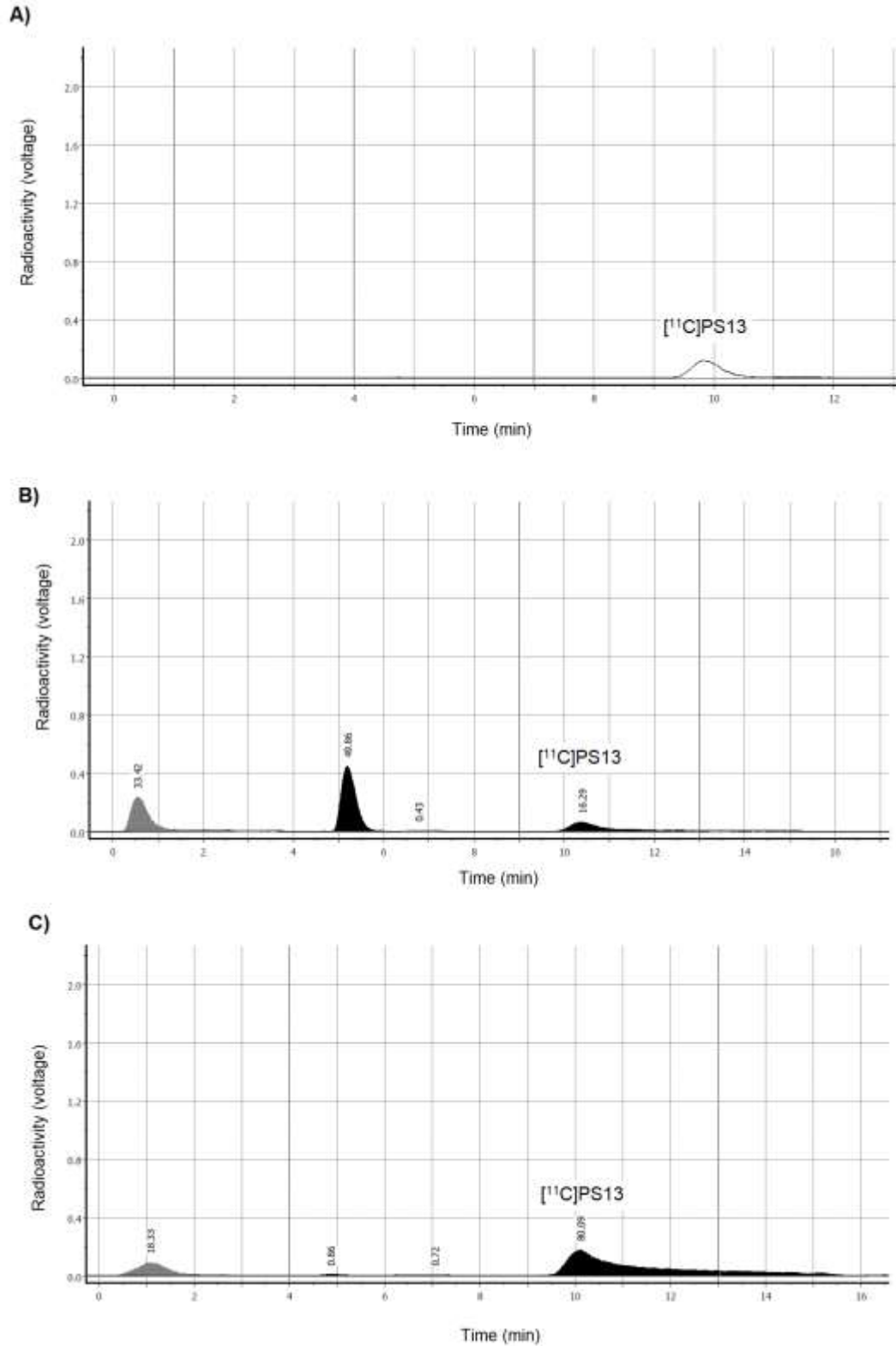
**SUPPLEMENTAL FIGURE 3.** *Ex vivo* biodistribution profile of [<sup>11</sup>C]PS13 in OVCAR-3 tumor-bearing mice (n=2, s.c. xenograft) with and without pre-treatment with ketoprofen. (A) shows the mean ± SD; (B) shows individual mouse data. Asterisks indicate significant differences (*p*<0.05).

**SUPPLEMENTAL TABLE 1.** Validation of PET data analyses of tumor (s.c. xenograft) radioactivity accumulation by *ex vivo* biodistribution studies. No significant differences were observed for tumor radioactivity accumulation results obtained from PET image analyses compared to biodistribution studies, and significant differences were observed between baseline and blocked tumor radioactivity accumulation results for both PET image analysis and biodistribution studies.

<b>TUMOR ACCUMULATION (%ID/G)</b>			
	<b>PET Analysis</b>	<b>Biodistribution</b>	<b><i>p</i></b>
<b>[<sup>11</sup>C]PS13<sub>40-60 MIN</sub></b>	3.56 ± 0.81 (n=6)	3.36 ± 0.48 (n=2)	0.76
<b>[<sup>11</sup>C]PS13 + KETOPROFEN<sub>40-60 MIN</sub></b>	1.30 ± 0.18 (n=2)	1.16 ± 0.12 (n=2)	0.46
<b><i>P</i></b>	0.00096	0.046	



**SUPPLEMENTAL FIGURE 4.** Radiometabolite analysis in a Mouse 1 (n=2) at 40 min p.i. with  $[^{11}\text{C}]\text{PS13}$ . (A) HPLC chromatogram of  $[^{11}\text{C}]\text{PS13}$  product following radiosynthesis; HPLC chromatogram with normalized peak analysis from (B) plasma and (C) tumor homogenate.



**SUPPLEMENTAL FIGURE 5.** Radiometabolite analysis in a Mouse 2 (n=2) at 40 min p.i. with  $[^{11}\text{C}]\text{PS13}$ . (A) HPLC chromatogram of  $[^{11}\text{C}]\text{PS13}$  product following radiosynthesis; HPLC chromatogram with normalized peak analysis from (B) plasma and (C) tumor homogenate.